Dissolved State of Atactic Polystyrene in Aromatic Solvents: Approaches through ¹H NMR, FT-IR and Adiabatic Compressibility

Kenji KAMIDE, Shigenobu MATSUDA, and Keisuke KOWSAKA

*Fundamental Research Laboratory of Fibers and Fiber-Forming Polymers,
Asahi Chemical Industry Co., Ltd.,
11–7, Hacchonawate, Takatsuki, Osaka 569, Japan*

(Received September 30, 1987)

ABSTRACT: An attempt was made to interpret significant differences in thermodynamic parameters, including the concentration dependence coefficients p_1 and p_2 of the polymer–solvent interaction parameter χ, Flory entropy parameter at infinite dilution ψ_0, Flory temperature θ, observed between atactic polystyrene (PS) in aromatic and aliphatic solvents by the characteristic features of the dissolved state of PS in aromatic solvents. For this purpose, ¹H NMR spectra were measured on PS/benzene, cyclohexane, toluene, and methylcyclohexane systems and the infrared spectra and adiabatic compressibility were determined for the former two solvents. In PS/aromatic solvents H_2-, H_3-, and H_4-phenyl proton peaks are shifted to a lower magnetic field than those in PS/aliphatic solvent, which was produced by hydrogenation of the aromatic solvent. The degree of solvation is slightly larger in benzene than in cyclohexane. The experimental results were explained only by the case where the PS phenyl ring was stacked in parallel to the solvent phenyl ring for PS/aromatic solvent systems.
    KEY WORDS   Polystyrene / Concentration Dependent Parameter / χ Parameter / Aromatic Solvent / ¹H NMR Spectrum / Planar Interaction / Chemical Shift / Infrared Spectrum / Adiabatic Compressibility /

Applying the Kamide–Matsuda[1] (KM) method to the critical solution point data (the critical polymer volume fraction $v_p{}^c$ and the critical temperature T_c) for fifteen systems of atactic polystyrene (PS) in a single solvent, Kamide *et al.*[1,2] determined the concentration dependent parameters p_1 and p_2 of the thermodynamic interaction parameter χ in the relation $\chi = \chi_0 (1 + p_1 v_p{}^+ p_2 v_p{}^2)$ (χ_0 is the concentration-independent coefficient, v_p, the polymer volume fraction), Flory temperature θ and Flory pair interaction entropy parameter ψ_0 at infinite dilution for these systems. To their results, they gave a brief discussion to explain the significant effect of solvent nature on solution properties of PS. For example, for PS/cyclopentane (CP), PS/cyclohexane (CH), and PS/methylcyclohexane

(MCH) systems, p_1 values for lower or upper critical solution points (LCSP or UCSP) are very similar to each other, but differences in ψ_0 values between CP and CH are much larger than those between CH and MCH for both CSP. From these analyses they concluded[2] that the skelton structure of the solvent is a more important factor than the substituent group to the skelton, covering the thermodynamic interaction between the polymer and solvent, and that even if the solvents have similar molecular weights and almost the same molecular shapes, p_1 and p_2 differ remarkably depending on whether the solvent is aliphatic or aromatic. Table I was made from Table II of ref 2 for p_1 and p_2 values, together with θ and ψ_0 of PS/CH, PS/benzene, PS/MCH, and PS/Toluene. For aliphatic

Table I. Concentration dependence of χ parameter p_1, p_2, Flory temperature θ, and entropy parameter ψ of polystyrene/single solvent system[1,2]

Solvent		p_1	p_2	θ/K	ψ
Cyclohexane	UCSP[a]	0.642	0.190	305.1	0.27
	LCSP[b]	0.638	−0.498	488.6	−0.58
Benzene	LCSP	0.388	−1.781	524.3	−1.81
Methylcyclohexane	UCSP	0.602	0.234	340.2	0.25
	LCSP	0.649	−1.183	487.9	−0.54
Toluene	LCSP	0.494	−0.922	550.4	−1.36

[a] Upper critical solution point.
[b] Lower critical solution point.

Table II. Temperature dependence of chemical shifts of polystyrene in aromatic and aliphatic solvents

Solvent	Temp/°C	Chemical shifts/ppm							
		Phenyl (H$_3$ and H$_4$)			Phenyl (H$_2$)			Methin	methylene
Benzene	20	7.08	7.05	6.95	6.73	6.62	6.48	2.09	1.59
	40	7.07	7.04	6.94	6.72	6.62	6.49	2.09	1.60
	60	7.06	7.04	6.93	6.71	6.62	6.50	2.10	1.61
	75	[7.07]	[7.03]	[6.95]	[6.71]	[6.60]	[6.49]	[2.09]	[1.61]
Cyclohexane	20	7.01	6.94	6.82	6.56	6.43	6.30	1.87	1.51
	30	6.99	6.94	6.82	6.56	6.44	6.30	1.87	1.51
	34.5	7.00	6.94	6.82	6.55	6.44	6.32	1.89	1.48
	40	7.00	6.94	6.81	6.56	6.44	6.33	1.89	1.47
	60[a]	6.99	6.94	6.82	6.55	6.44	6.34	1.89	1.47
	75	[6.99]	[6.94]	[6.82]	[6.68]	[6.57]	[6.35]	[1.92]	[1.48][b]
(B-CH)[c]	60	0.07	0.10	0.11	0.16	0.18	0.16	0.21	0.13
Toluene	20	7.1[b]	7.0[b]	6.92	6.68	6.58	6.43	2.04	1.57
	40	7.1[b]	7.0[b]	6.92	6.68	6.58	6.44	2.05	1.58
	60[a]	7.07	7.01	6.91	6.69	6.58	6.46	2.06	1.59
	75	[7.1][b]	[7.0][b]	[6.91]	[6.68]	[6.57]	[6.45]	[2.05]	[1.59]
Methylcyclohexane	40	6.99	6.94	6.82	6.55	6.45	6.36	1.90	1.5[b]
	70	6.99	6.95	6.82	6.56	6.45	6.36	1.91	1.5[b]
	78	6.99	6.94	6.82	6.56	6.47	6.36	1.91	1.5[b]
	90[a]	6.99	6.94	6.81	6.57	6.49	6.37	1.93	1.54
(T-MCH)[d]	60, 90	0.08	0.07	0.10	0.12	0.09	0.09	0.13	0.05

[a] Eliminated solvent peak by double pulse sequence.
[b] Overlapped with solvent peak.
[c] Difference of chemical shifts between PS/benzene and PS/CH.
[d] Difference of chemical shift between PS/toluene and PS/methylcyclohexane.
[ ] were measured by JNM-FX400.

solvent systems (PS/CH and PS/MCH), p_1 for LCSP was found to be 0.64—0.65, being near the theoretically expected value (2/3[2,3]) for non-polar polymer/non-polar solvent system, in which the molecular forces acting between the solute and the solvent is only dis-

persion force. These values also coincide with the averaged p_1 value (0.638 ± 0.035^2) of twelve PS/solvent systems. In contrast to this, for PS/benzene and PS/toluene systems p_1 for LCSP was 0.39 and 0.49, respectively. These results seem surprising because for these solutions the polymer repeating unit has a similar chemical structure with solvents and minimum deviation, if any, of the free energy change in mixing from that of random mixing athermal solution is expected. In addition to this, if we consider that benzene and toluene are practically non-polar and CH and MCH are less polar, it seems very curious that there are large differences in thermodynamic properties between PS/aromatic and PS/aliphatic solvents.

Kamide et al.[2] were probably the first to interpret the above findings in terms of the molecular dissolved state of polymer: They measured PS/CH and PS/benzene-d_6 ^{1}H NMR spectra using a less resolving power NMR spectrometer (60 MHz JEOL NMR spectrometer type PMX60), finding a significant shift of the proton peak of the phenyl group constituting PS molecules dissolved in benzene-d_6 toward lower magnetic field. They gave the following explanation for the above experimental findings: The magnetic shielding effect induced by circular electric current is strengthened by planar interaction between the benzene ring of PS and benzene as solvent and this interaction makes benzene a better solvent than CH.[2]

Fujihara[4] determined using a Ness type (dilution type) constant temperature wall calorimeter the heat of dilution of PS/CH and PS/benzene systems showing that PS/CH is endothermic but PS/benzene is small, but significantly exothermic and as a result, the latter system is expected to be more stable than the former. Fujihara[4] also speculated in his interesting dissertation the formation of the alternatively overlapping structure of the phenyl ring of PS and benzene as solvent unfortunately without any experimental evidence,

which may lead to stability to the system.[4] Except for a few attempts, no specific consideration has not been paid up to now to specific interactions between PS molecules and aromatic solvents. This motivated our further research:

In this article, we (1) disclose the solvent effect of the chemical shifts of protons, assigned to phenyl, methin, and methylene of PS, in more detail by measuring more accurately ^{1}H NMR spectra for atactic PS/CH, atactic PS/benzene, atactic PS/MCH and atactic PS/toluene systems with reexamination of the adequacy of the assignment of each peak in phenyl envelope in observed NMR spectrum, (2) examine the solvent effect of PS/aromatic solvent systems by measuring IR spectra of atactic PS/CH and atactic PS/benzene systems, and (3) evaluate the effect of solvent nature (aliphatic or aromatic) on the degree of solvation by determining the adiabatic compressibility of these systems.

EXPERIMENTAL

Polymer Sample and Solvents

As an atactic PS sample a whole polymer of a commercially available product with the trade name of Styron 666 (Asahi Chemical Industry Co., Ltd.) was employed without further fractionation. The polymer has a weight-average molecular weight $\bar{M}_w$ of 23.9×10^4 by gel permeation chromatography (GPC) with tetrahydrofuran (THF) and a 23.2×10^4 by light scattering with benzene at $25°C$[5] and has a number-average molecular weight $\bar{M}_n$ of 8.6×10^4 by GPC with THF and of 8.9×10^4 by membrane osmometry with toluene at $25°C$.[5]

Deuterated CH, benzene, MCH and toluene (CH-d_{12}, benzene-d_6, MCH-d_{14}, and toluene d_8), manufactured by E. Merck Inc. (West Germany), were used as received as solvents for NMR measurements. For adiabatic compressibility measurements, reagent grade CH and benzene, manufactured by Wako Pure

K. KAMIDE, S. MATSUDA, and K. KOWSAKA

Chemical Industries Ltd. (Osaka), were used as received.

^1H NMR Spectroscopy

^{1}H NMR measurements were made on FT-NMR (JEOL, JNM-FX400 and JNM-FX200) spectrometers at 400.5 and 199.5 MHz under the following operating conditions: Polymer concentration, 1.0 wt%; temperature, 20—75°C (PS/benzene-d_6, PS/CH-d_{12} and PS/toluene-d_8) and 40—90°C (PS/MCH-d_{14}); ^{1}H pulse width, 6 μs (45° pulse); spectral width, 8000 Hz (ca. 20 ppm) and 2000 Hz (ca. 10 ppm); data points 16384; repetition time 3 s and 10 s; accumulation, 8 and 16 times. The chemical shifts were determined using tetramethylsilane (TMS) as the internal reference. For PS/toluene-d_8, PS/CH-d_{12} and PS/MCH-d_{14} systems, there exists a peak due to protons remaining in the solvent, near the proton peaks of PS and for this reason, the 7 chemical shifts of PS were determined in addition to the internal reference material method, by eliminating the solvent peak with the π-τ-$\pi/2$-FID (free induction decay) pulse method. Here, τ was estimated by trial and error over a range of 5—9 s and the repetition time was 30 s and accumulation was 8 times.

Spin-lattice relaxation time T_1 and chemical shift of CH and benzene were measured, employing two coaxially centered sample tubes. Deuterium oxide (D_2O) was employed as external lock solvent. Solvent (CH or Benzene) or solution (PS/CH or PS/benzene) was placed in the inner tube. By the inversion-recovery method using π-τ-$\pi/2$-FID pulse sequences, the peak intensity of the solvent peak was determined at various intervals τ. T_1 can be evaluated from the following equation,[6]

$$\tau/T_1 = -\ln\{(A_{150s} - A_\tau)/2A_{150s}\} \qquad (1)$$

where A_{150s} and A_τ represent peak intensity of the solvent peak at intervals of 150 s and τ.

Infrared Spectroscopy

Infrared spectra of PS/CH(polymer con-centration $c = 10$ wt%), PS/benzene ($c = 10$ wt%) and benzene/CH were measured on a FT-IR spectrometer (JEOL, JIR-3505) using a conventional dismantlable cell without spacers (capillary method). The resolving power was 2 cm^{-1}.

Adiabatic Compressibility

The ultrasonic velocity V was measured in PS/CH at 40°C and PS/benzene at 25°C using a sing-around method on a Nusonic 6080 sound velocity measuring apparatus (Mapco Inc., U.S.A). The temperatures of the solutions were controlled to ± 0.005°C. The density ρ of the solution was measured by an Ostwald type pycnometer.

RESULTS AND DISCUSSION

Figure 1a and b show 200 MHz ^{1}H NMR spectra of PS/benzene-d_6 and PS/CH-d_{12} both at 60°C and Figure 2a and b show 200 MHz ^{1}H NMR spectra of PS/toluene-d_8 at 60°C and PS/MCH d_{14} at 90°C. In these spectra phenyl, aliphatic methin, and methylene protons are observed over 6.3—7.2 ppm, 1.8—2.2 ppm, and 1.4—1.7 ppm, respectively. The spectra in the phenyl proton region are split into two envelopes. Figure 3a and b demonstrate 400 MHz ^{1}H NMR spectra of the phenyl proton region of PS/benzene-d_6 and PS/toluene-d_8 at 75°C. Harwood and Shepherd[7] assigned at a lower magnetic field in two phenyl proton envelopes to H_3-protons and at higher magnetic field in that envelope to H_2-proton. Since the integrated intensity ratio of these two peaks is approximately 3:2, it is clear that the H_4-proton envelope ovelaps with the H_3-proton envelope. The validity of the above assignment of the chemical shift of H_4-proton was also confirmed by Carbon-Hydrogen shift correlation NMR spectroscopy (not shown here). In addition, the H_2-proton envelope clearly consists of three components. This indicates that H_2-proton peak are splits according to stereochemical differ-
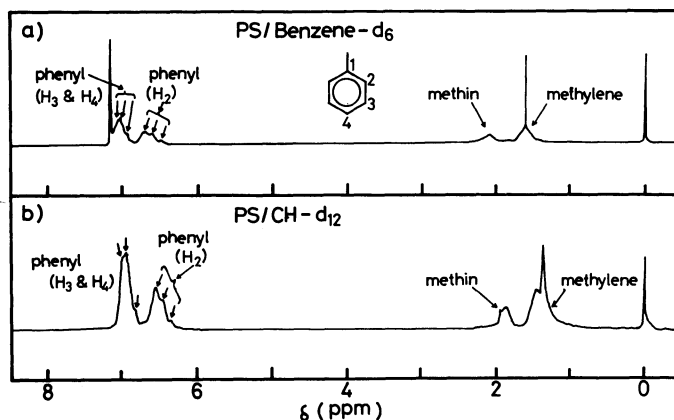
Figure 1. 200 MHz ^{1}H NMR spectra of atactic polystyrene in benzene-d_6 (a, 60°C) and in cyclohexane-d_{12} (b, 60°C).
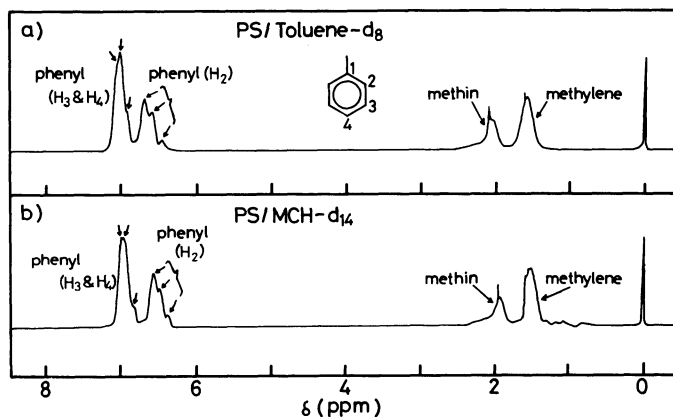

Figure 2. 200 MHz ^{1}H NMR spectra of atactic polystyrene in toluene-d_6 (a, 60°C) and in methylcyclohexane-d_{14} (b, 90°C).

ence. In this case vicinal proton coupling is considered below 10 Hz (0.05 ppm)[6] and is of the order of the line width and accordingly, splitting due to this coupling is not observable. Inspection of ^{1}H NMR spectra for isotactic and atactic PS reported by Inoue *et al.*[8] in tetrachloroethylene at 120°C (Figure 1 of ref 8) shows that the H_2-proton region of isotactic PS falls fairly well in a region in the H_2-proton peak of atactic PS. Therefore, among three peaks constituting the H_2-proton envelope, a peak at lowest magnetic field can be assigned as an iso(*mm*)-peak (here, *m* means *meso* con-

figuration) and the remaining two peaks can be attributed to hetero(*mr* or *rm*)- and syndio(*rr*)-peaks (*r* is *racemo* configuration). Similar splitting is also expected to occur in H_3- and H_4-proton envelopes and in fact, more than 3 peaks are observed, but the degree of splitting is explicitly low. It can be considered that, due to the higher electron density of H_2 proton as compared with H_3 and H_4 protons, the H_2 proton region in ^{1}H NMR spectra is sensitive to the configuration of PS, splitting into roughly three parts. H_3- and H_4-envelopes in PS/benzene-d_6 are, more or less, unavoidably
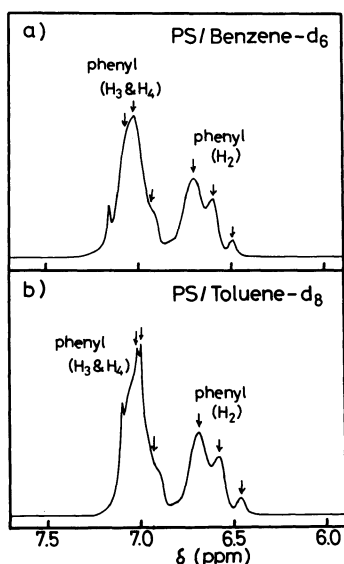
235

Figure 3. 400 MHz ^{1}H NMR spectra of the phenyl proton region of atactic polystyrene in benzene-d_6 (a) and in toluene-d_8 (b), both at 75°C.

overlap with solvent benzene peaks. In this article, as far as H_3- and H_4-envelopes are concerned the main three peaks observed commonly in all the solvents investigated were analyzed further. Table II shows the chemical shifts of phenyl, methin and methylene peaks of PS in four solvents at various temperatures. In PS/benzene-d_6, H_3- and H_4-phenyl proton peaks shift by 0.07—0.11 ppm to a lower magnetic field and H_2-phenyl proton peaks by 0.16—0.18 ppm to a lower magnetic field than those in PS–CH-d_{12}. Similarly, H_3- and H_4-phenyl proton peaks and H_2-phenyl proton peaks in PS/toluene-d_8 shift by 0.08—0.10 ppm and by 0.09—0.12 ppm, respectively, to a lower magnetic field than those in PS/MCH-d_{14}. Methin and methylene peaks of PS in aromatic solvents are found at a lower magnetic field than those of PS in aliphatic solvents. Differing from aliphatic solvents, aromatic solvents exhibit naturally anti-magneticism without exception and this anti-magnetic field originating from the aromatic solvent also reaches TMS. Then, the effects of anti-magneticism of the aromatic solvent on the whole NMR spectra luckily cancell out each other and are neglected here. This suggests strongly that a significant shift of the ^{1}H NMR-peaks of H_2-, H_3-, and H_4-phenyl protons, and methin and methylene protons in aromatic solvents to a lower magnetic field as compared with those in aliphatic solvents can only be explained by taking into consideration the specific interaction between phenyl rings of PS and benzene as solvent.

Benzene is a non-polar, but is said to have partly regular structure in the liquid state due to "π-π" electrostatic interactions originating from overlapping of π electron orbitals of benzene molecules. In fact, the molecular orbital calculation[9] with assumption of C_{2v} symmetry of energy levels of π electrons in benzene, when two neighbouring benzene molecules are packed together like a sheet, shows the splitting of each energy level into two, whose distance from the original state equals the interaction energy between two neighbouring benzene rings and the π electron of overlapping benzene transits naturally to a lower level, which is of course lower than that of a single benzene molecule. Accordingly, liquid benzene may be stabilized by taking, at least partly, the planarly overlapping structure. It is confirmed with experiments of the small-angle X-ray diffraction from liquid benzene that liquid benzene maintains to some extent such a planary overlapping structure observed originally in benzene crystals.[10]

In order to examine the specific interaction between benzene and PS, IR spectra for benzene/CH, PS/CH system were measured. Theoretically, only four vibrations are expected to be observed at 673 (A_{2u}), 1038 (E_{1u}), and 3063 cm^{-1} (E_{1u}), due to the structural symmetry of benzene molecule (D_{6h}) and in fact this is confirmed for gaseous benzene. In the liquid state, the structural symmetry is destroyed partly, resulting in numerous absorption bands such as those at 1448, 1531, 1815, 1960, 3035, and 3095 cm^{-1}, which are forbidden in the gas state, become observ-
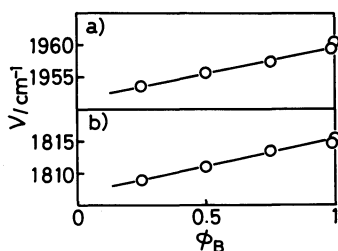
Figure 4. Wave numbers v of IR spectrum of liquid benzene/CH system with various molar fractions of benzene ϕ_B.

Figure 5. IR spectrum of PS film (a) and subtracted IR spectra of PS from PS/CH (b) and from PS/benzene (c) systems.

able.[11] Figure 4 shows the plot of two absorbing wave numbers v, due to out-of-plane vibrations (1815 and 1960 cm^{-1} for pure liquid benzene), as a function of the molar fraction of benzene ϕ_B. All other absorption bands remained constant within experimental uncertainty regardless of ϕ_B. These two absorption peaks are considered to be peaks that are combined in the following ways[12]:

$$1815\,\text{cm}^{-1} = 975\,\text{cm}^{-1} + 849\,\text{cm}^{-1} \qquad (2)$$

and

$$1960\,\text{cm}^{-1} \simeq 975\,\text{cm}^{-1} + 995\,\text{cm}^{-1} \qquad (3)$$

The absorption bands at 849 (E_{1g}), 975 (E_{2u}), and 995 cm^{-1} (B_{2g}) are assigned for out-of-plane vibration originally forbidden in IR spectra and became observable by the existence of an interaction working perpendicularly to the benzene-ring surface. Inspection of Figure 4 leads to the conclusion that the interaction between benzene molecules, which is also expected from analysis of small angle X-ray diffraction experiments of liquid benzene,[10] is weakened by dilution of benzene with CH.

Figure 5 shows the subtracted IR spectra, which are obtained by subtracting IR spectrum of CH from that of PS/CH system ($c = 10\,\text{wt}\%$) (b) and by subtracting IR spectrum of benzene from that of PS/benzene ($c = 10\,\text{wt}\%$) (c), respectively. For the former spectrum, the absorption band at 2927 cm^{-1} intrinsic to CH was used as the standard peak
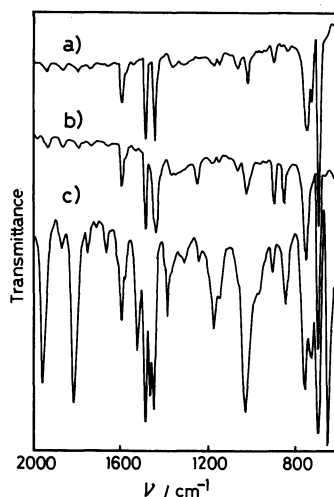
so that transmittance at 2927 cm^{-1} becomes zero for the subtracted spectrum, and for the latter the absorption band at 675 cm^{-1} was used as the standard peak. In the figure, IR spectra of solid PS are shown for comparison (a). It is interesting to note that the difference spectrum (PS/CH–CH) have almost the same IR spectrum of PS, but the difference spectrum (PS/benzene–benzene) has a large number of very complicated, additional bands, including out-of-plane vibrations for pure liquid benzene (1815 and 1960 cm^{-1}), besides the original PS bands. This experimental result implies that an interaction between PS molecule and benzene brings about the appearance of new absorption bands, which are observed in neither PS nor benzene, and/or significant shifts of the absorption bands of PS or benzene. In this way, analysis of IR spectra shows the existence of a specific interaction between PS and benzene.

In contrast to benzene, only a dispersion force is working in CH. CH has molecular shape and molecular size both similar to benzene, but CH has a density smaller by 0.1 (g/cm^{-3}) than benzene at room temperature, indicating that liquid CH is expected to have

no regular structure and a larger free volume than benzene.

Possible solvent effects on the polymer proton chemical shifts are the effect due to change in molecular chain conformation with solvent nature and the effect of shielding or deshielding magnetically the solute molecule by the solvent molecule. Hereafter, we discuss the latter effect only.

It can be regarded that liquid CH and methylcyclohexane (MCH) have little magnetic anisotropy and no hydrogen bonding, resulting in neither shielding nor deshielding effects on the solute polymer. In addition, a chemical shift of reference material (in this case TMS) is influenced by solvent to the same degree as those of the solute molecule and then an insignificant effect on aliphatic hydrocarbons such as CH and MCH on the PS chemical shift is expected. On the other hand, a significant shift of the chemical shifts of all protons (including H_2-, H_3-, H_4-, methin, and methylene protons), of PS dissolved in aromatic solvents, to a lower magnetic field as compared with those in aliphatic solvents indicates some specific interactions between PS and aromatic solvents.

In the phenyl ring of benzene and toluene, placed in the static magnetic field H, the π electron moves circularly along the ring (ring current effect) and as a result the solvents show a strong anti-magnetic effect perpendicular to the ring plane (Figure 6a). The protons in the vicinity of the ring surface shift to a higher magnetic field due to the shielding of H' and protons near outside of the ring edge are shifted to a lower magnetic field by deshielding effect (Figure 6b). Here, to the region in which deshielding effect is effective, solvent molecules are not accessible due to steric interference of the proton and in the case when the aromatic solvents are randomly mixed with the solute molecules, a major part of the solute molecules is influenced by the shielding effect, resulting in a higher magnetic field shift of the proton chemical shifts. Conversely, the ex-
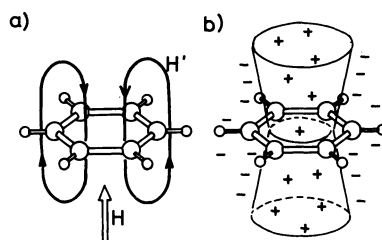

Figure 6. Schematic representation of a phenyl ring under external magnetic field (H): (a) anti-magnetic field (H') of a phenyl ring; (b) shielded area (+) and deshielded area (−) of a phenyl ring.
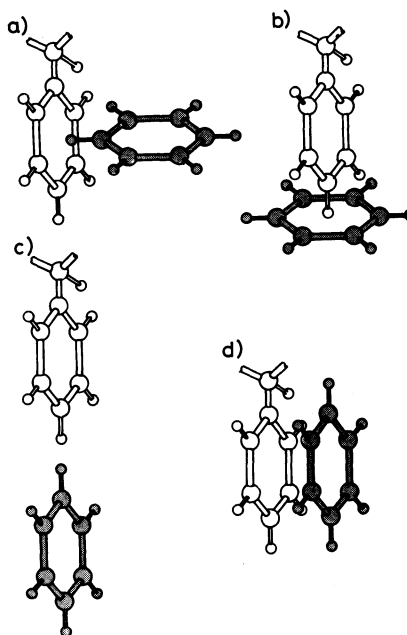

Figure 7. Schematic representation of four types of possible coordination of the solvent phenyl ring with the PS phenyl ring.

perimental fact that the proton chemical shifts of PS show lower magnetic field shift in aromatic solvents suggests that the solvent molecules are selectively coordinated in a manner such that the solvent molecules exert mainly deshielding effect against PS molecules.

Four types of coordination of the solvent phenyl ring toward PS may be possible as shown in Figure 7. The case when the PS phenyl ring perpendicular to the solvent

phenyl ring (Figure 7a and b), the PS protons are not influenced by deshielding effect. These cases, then, should be discarded for PS-aromatic solvent system. The case when PS phenyl ring and the solvent phenyl ring are placed side by side on the same plane (Figure 7c), the peak of the protons existing between two phenyl rings is expected to shift slightly to a lower magnetic field by strengthening the anti-magnetic field between two phenyl rings, but this coordination type cannot explain the lower magnetic field shift of methin and methylene proton peaks. In the case when the PS phenyl ring is stacked in parallel to the solvent phenyl ring (Figure 7d), the magnetic field H' brought about from circular electric current of the PS phenyl ring and the magnetic field H'' from the solvent phenyl ring deshield strongly the PS phenyl protons (Figure 8b), resulting in their chemical shifts to a lower magnetic field and in addition, as Figure 8 clarifies, the magnetic field H' + H'' brings about a lower magnetic field shift of methin and methylene peaks. Therefore, among these four coodination types, the experimental results of ^{1}H NMR spectra can be interpreted only by the case where the PS phenyl ring is stacked in parallel to the solvent phenyl ring. This model may be accepted by speculation that an addition of PS to benzene causes partial destruction of the benzene–benzene planar stacking-in-sheets-structure in benzene liquid and formation of the benzene–PS phenyl ring overlapping structure.

When PS is dissolved in CH, the formation of regular structure cannot be expected. To PS/toluene and PS/MCH systems, the above discussion will also be applied. Figure 8 illustrates the difference between aromatic and aliphatic solvents in the magnetic interaction against PS. Here H is an external magnetic field. The experimental fact that the differences of the chemical shifts between benzene-d_6 and CH-d_{12} are always larger than those between toluene-d_{12} and MCH-d_{14} (see Table II) might be interpreted in terms of better molecular
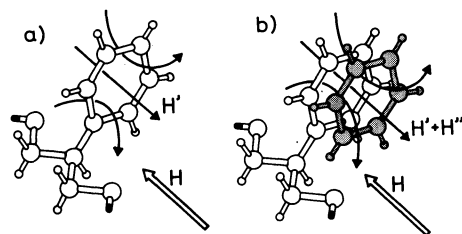

Figure 8. Schematic representation of polystyrene repeating unit under an external magnetic field (H): (a) polystyrene in an aliphatic solvent, (b) polystyrene in an aromatic solvent.

Table III. ^{1}H and ^{13}C NMR spin-lattice relaxation time T_1 and the chemical shift of solvent proton for cyclohexane, benzene and their solutions of polystyrene ($\bar{M}_w = 1.00 \times 10^4$) at 40°C

Sample	^{1}H		^{13}C	
	T_1/s	δ/ppm[a]	T_1/s	δ/ppm[a]
CH	4.07	1.44	19.89	27.27
CH with PS	3.85	1.43	17.09	27.61
Benzene	6.55	7.15	27.14	128.58
Benzene with PS	6.34	7.15	24.59	128.48

[a] TMS (= 0 ppm) internal reference.

symmetry of benzene-d_6, which brings about stronger circular electric current resulting in larger H''. The methin and methylene protons are surrounded by the benzene ring of PS and may be also affected by H'', resulting in a lower magnetic field shift when dissolved in aromatic solvents.

The ^{1}H and ^{13}C NMR spin lattice relaxation time T_1 as well as the chemical shift of solvent proton for CH, benzene and their solutions of a monodisperse PS with $\bar{M}_w = 1.00 \times 10^4$ (concentration, 0.1 g PS/1.0 ml solvent) are shown in Table III. It is evident that some liquid structures of CH and benzene are slightly destroyed addition of PS molecules. But the degree of destruction is comparatively small. For example, we have observed that T_1 of water (1.6 s) decreased, by addition of sodium hydroxide to produce 10 wt% aq. sodium hydroxide, to 0.98 s and also decreased, by ad-
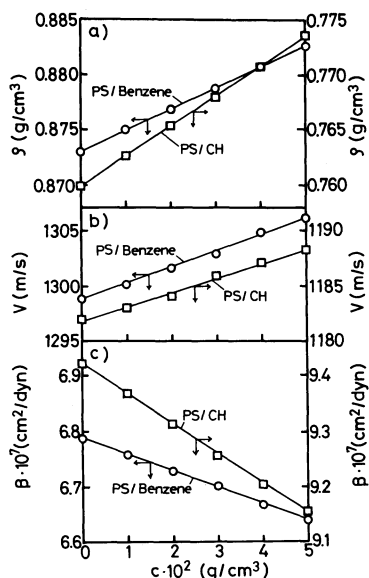
Figure 9. Plots of density ρ (g cm^{-3}), sound velocity V (m s^{-1}), and adiabatic compressibility β (cm^2 dyn^{-1}) vs. concentration c (g cm^{-3}) of polystyrene/benzene (O, 20°C) and polystyrene/cyclohexane (□, 40°C) solutions.
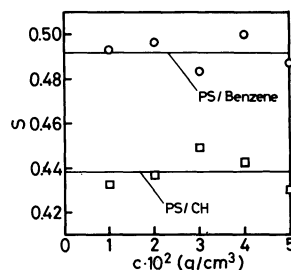

Figure 10. Number of solvated solvent molecules per repeating unit of polystyrene for polystyrene/benzene (O, at 20°C) and polystyrene/cyclohexane (□, 40°C) at various concentrations c (g cm^{-3}).

dition of cellobiose to produce 10% solution, to 1.0 s.[13]

Figure 9a and b show the concentration (c) dependence of the density ρ, and the sound velocity V of PS/CH at 40°C and PS/benzene at 20°C. Both ρ and V increase linearly with increase in c.

Adiabatic compressibility β was calculated through Laplace's equation

$$\beta = \frac{1}{\rho V^2} \qquad (4)$$

from ρ and V values. β is plotted agaist c in Figure 9c. β decreases in linear proportion to c.

The gram of solvated solvent molecules per gram of polymer n is given by[14]

$$n = \left(1 - \frac{\beta}{\beta_0}\right)\frac{100\rho - c}{c} \qquad (5)$$

where β_0 is β of the pure solvent. n can be readily transformed into the number of solvated solvent molecules per repeating unit of the polymer (S) by

$$S = \frac{m_p}{m_s} n \qquad (6)$$

Here, m_p and m_s are the molecular weights of the polymer repeating unit and the solvent, respectively. Figure 10 shows the concentration dependence of S for PS/benzene at 20°C and PS/CH system at 40°C. S is roughly constant independent of c. S at infinite dilution (S_0) was found to be 0.49 for PS/benzene and 0.44 for PS/CH, indicating that the degree of solvation is very low but slightly larger in benzene than in CH. The experimental error of sonic velocity and density measurements are estimated to be ± 1 m^{-1}s and 5×10^{-4} g cm^{-3}, respectively, and for PS solutions S and accordingly S_0 can be determined with a relative error of ± 0.17. Therefore, the values estimated here ($S_0 = 0.49$ for PS/benzene and $S_0 = 0.44$ for PS/CH) indicate that the solvation occurs, although to less extent, significantly. These S_0 values should be compared with those (2.0—3.0) determined for cellulose acetates dissolved in polar solvents.[15]

The experimental facts that p_1 values of PS/benzene and PS/toluene are about 30—40% smaller than the theoretically expected value for non-polar polymer/non-polar solvent and the absolute magnitude of the Flory entropy parameter ψ_0 of these systems are almost 3 times larger than those for PS/CH and PS/

MCH (Table I) seem to be closely coorelated not with the number of solvated molecules per repeating unit molecule, but with the way of the solvation; that is, the specific feature of PS/aromatic solvent system may be caused by planar interaction between PS phenyl group and benzene ring of the solvent. At present time, we cannot reach to the final and quantitative explanation for the change in p_1 and ψ_0 in terms of solute–solvent interaction, but we can easily consider that p_1 for PS/aromatic solvent systems deviates from the theoretically expected value.

Summarizing the analyses of ^{1}H NMR spectrum and adiabatic compressibility of several PS/aromatic solvent and PS/aliphatic solvent systems, there some planar interactions occur between PS and aromatic solvent molecule, which may cause a significant difference from the PS/aliphatic solvent system.

REFERENCES

1. K. Kamide and S. Matsuda, *Polym. J.*, **16**, 825 (1984).
2. K. Kamide and S. Matsuda, and M. Saito, *Polym. J.*, **17**, 1013 (1985).
3. M. Kurata, "Thermodynamics of Polymer Solutions," Harwood Academic Publishers, Chur, London, New York, 1982.
4. I. Fujihara, Ph. D. Dissertation, 1979, Osaka City Univ.
5. K. Kamide, Y. Miyazaki, and T. Abe, *Makromol. Chem.*, **177**, 485 (1976).
6. See, for example, R. Abraham and P. Loftus, "Proton and Carbon-13 NMR Spectroscopy," John Wiley & Sons, Inc., New York, N. Y., 1978, Chapters III and VI.
7. H. J. Harwood and L. Shepherd, unpublished results cited in D. Y. Yoon and P. J. Flory, *Macromolecules*, **10**, 562 (1977).
8. Y. Inoue, A. Nishioka, and R. Chûjô, *Makromol. Chem.*, **156**, 207 (1972).
9. J. D. Roberts, "Note on Molecular Orbital Calculation," W. A. Benjamin Inc., New York, N. Y., 1962; Y. Yukawa, R. Mikawa, and K. Itoh, "Exercises in Molecular Orbital Calculations," Hirokawa Pub., Co., Tokyo, 1965.
10. See, for example, A. H. Narten, *J. Chem. Phys.*, **48**, 1630 (1968).
11. C. Bailey, C. Ingold, H. Poole, and C. Wilson, *J. Chem. Soc.*, 222 (1946).
12. R. Mair and G. Hornig, *J. Chem. Phys.*, **17**, 1236 (1949).
13. T. Yamashiki, K. Kamide, K. Okajima, K. Kowsaka, T. Matsui, and H. Fukase, submitted to *Polym. J.*
14. A. Passynsky, *Acta Physicochim. U.S.S.R.*, **22**, 137 (1974).
15. K. Kamide and M. Saito, *Eur. Polym. J.*, **20**, 903 (1984).